Cellular Physiology and Biochemistry

Cell Physiol Biochem 2017;43:94-107
DOI: 10.1159/000480322
Published online: August 25, 2017
Accepted: June 22, 2017

Original Paper

CyclinG1 Amplification Enhances Aurora Kinase Inhibitor-Induced Polyploid Resistance and Inhibition of Bcl-2 Pathway Reverses the Resistance

Wenfeng Zhang[a] Jie Xu[b,c] Dexiang Ji[d] Zhangyun Li[e] Wenxing He[f] Fei Yang[g] Huiyin Lan[g] Yu Wang[h] Zhengping Wu[a] Xiaoshan Liu[a] Shanhua Huang[a] Longkun Li[c] Weihua Zhou[b]

[a]Department of Infectious Disease, the First Affiliated Hospital, Nanchang University, Nanchang, [b]Department of Oncology, the Second Affiliated Hospital, Nanchang University, Nanchang, [c]Department of Urology, the Second Affiliated Hospital, Third Military Medical University, Chongqing, [d]Department of Hematology, the First Affiliated Hospital, Nanchang University, Nanchang, [e]Department of Oncology, the Third Hospital of Nanchang, Nanchang, [f]Department of Breast Surgery, Jiangxi Province Tumor Hospital, Nanchang, [g]Institute of Translational Medicine, Zhejiang University, Hangzhou, [h]Department of Nephrology, the First Affiliated Hospital, Nanchang University, Nanchang,, P.R. China

Key Words
CyclinG1 • Polyploidy • Resistance • Bcl-2 family • Targeted therapy • Breast Cancer

Abstract
Background/Aims: CyclinG1 (CycG1) is frequently overexpressed in solid tumors and overexpression of CycG1 promotes cell survival upon paclitaxel exposure by inducing polyploidy. Whether and how CycG1 regulates polyploidization caused by small molecular targeted inhibitors remains unclear. ***Methods:*** Immunohistochemistry and immunoblotting were utilized to examine protein expression. Cell proliferation was measured by ATPlite assay, and cell cycle distribution and apoptosis were measured by flow cytometry and/or DNA fragmentation assays. ***Results:*** Overexpression of CycG1 in breast cancer cells caused apoptosis-resistant polyploidy upon treatment with Aurora kinase inhibitor, ZM447439 (ZM). Addition of ABT-263, a small-molecule BH3 mimetic, to ZM, produced a synergistic loss of cell viability with greater sustained tumor growth inhibition in breast cancer cell lines. Decrease of Mcl-1 and increase of NOXA caused by ZM treatment, were responsible for the synergy. Furthermore, CycG1 was highly expressed in Triple-Negative-Breast-Cancer patients treated with paclitaxel and was paralleled by decreased cell survival. ***Conclusion:*** CycG1 is a crucial factor in ZM-induced polyploidy resistance, and ABT-263/ZM combination hold therapeutic utility in the CycG1-amplified subset of breast cancer and CycG1, thus, is a promising target in breast cancer

W. Zhang and J. Xu contributed equally to this work.

Weihua Zhou
and Longkun Li

Department of Oncology, the Second Affiliated Hospital, Nanchang University, Nanchang, 330006 (P.R. China); Department of Urology, the Second Affiliated Hospital, Third Military Medical University, Chongqing, 400037 (P.R. China)
E-Mail juliazhouwh@gmail.com / lilongk@hotmail.com

KARGER

Introduction

CyclinG1 (CycG1), also known as CCNG1, was firstly identified as a member of cyclin family with homology to c-src [1], and was further found to be a transcriptional target of p53 [2]. Moreover, CycG1 negatively affects the stabilization of p53 by promoting protein degradation through a negative feedback signaling to the p53-MDM2 auto-regulatory module [3, 4]. The precise role of CycG1 on cellular growth is still controversial. CycG1 overexpression promotes cancer cell growth [5-7], which is suppressed by CycG1 antisense constructs [8-10]. Consistent with these data, CycG1 is frequently overexpressed in human breast and prostate cancers [11], osteosarcoma [12], colorectal tumor cells [13] and hepatocellular carcinoma [14], showing close correlation with distant metastasis and poor prognosis. Conversely, the induction of CycG1 after DNA damage and its role in G_2-M arrest suggest a possible growth inhibitory activity [5, 15], which is possibly dependent on the magnitude of CycG1 expression [16]. Indeed, CycG1 is still dominantly suggested as a growth promotion factor rather than arrest factor.

CycG1 does not pair with a known cyclin-dependent kinase, and thus, its biological functions are likely distinct, and remain to be fully elucidated. Recently, CycG1 has been identified to play a novel role in regulation of polyploidy and resistance to chemotherapy. Cells exposed to anti-mitotic drugs usually arrest in pro-metaphase for a prolonged period, whereas they eventually exit mitosis and enter the next G_1 as 4N or 8N DNA polyploidy cells in a process known as mitotic "slippage", which requires the ubiquitylation and proteolysis of Cyclin B1 (CycB1), or stop dividing and undergo senescence, or activate pathways that lead to cell death [17-20]. Increased CycG1 expression accompanies paclitaxel-induced mitotic arrest and promotes cell survival after paclitaxel exposure, whereas CycG1 depletion by RNA interference delays mitotic slippage and enhances paclitaxel-induced apoptosis [21]. Furthermore, overexpression of CycG1 inhibits cytokinesis in neonatal cardiomyocytes and leads to an enlarged population of binuclear cardiomyocytes whereas inactivation of CycG1 in mice lowers the degree of polyploidy and multinucleation in cardiomyocytes [22]. These data show that CycG1 represents a novel factor regulating the poorly characterized polyploidylation processes.

Here, we aim to investigate the role of CycG1 in regulation of polyploidy induced by small molecular targeted inhibitor in breast cancer cells, and demonstrate whether CycG1 is a potential anti-cancer target in breast cancer. To this end, we find that Aurora kinase inhibitor ZM447439 (ZM) induces mitotic slippage and apoptosis-resistant polyploidy cells in CycG1-amplified breast cancer cells, whereas triggers apoptosis in CycG1-low-expressed breast cancer cells. ABT-263, a small-molecule BH3 mimetic, induces the rapid demise of ZM-induced polyploidy cells in CycG1-amplified cells. Furthermore, overexpression of CycG1 is found in paclitaxel-treated triple negative breast cancer (TNBC) tissues and associates with inferior survival. Our data suggest that CycG1-amplification is responsible for ZM-induced resistant polyploidy and combination of ZM and ABT-263 could be a promising strategy for CycG1-amplified breast cancer therapy. CycG1, thus, is a promising target in breast cancer.

Material and Methods

Reagent and cell culture

ZM447439 (Santa Cruz), MLN8237 (Selleck Chemicals) and ABT-263 (Santa Cruz) were dissolved in dimethyl sulfoxide (DMSO) and stored at -20°C. Human MDA-MB-231, MDA-MB-361, MDA-MB-468, ZR-75-1, MCF7, and SKBR3 cell lines were obtained from the American Type Culture Collection (ATCC). ZR-75-1 was grown in RPMI-1640 medium supplemented with 10% FBS and the other five cell lines were grown in DMEM medium supplemented with 10% FBS. Cells were cultured at 37°C in a humidified atmosphere containing 5% CO_2. Control cultures received an equivalent amount of DMSO only.

Immunoblotting (IB) and antibodies

For direct IB analysis, cells were lysed in a Triton X-100 or RIPA buffer with phosphatase inhibitors. The antibodies used were as follows: HA (1:2000; Roche), CycG1 (1:500; Santa Cruz), PARP (1:1000; Cell Signaling), Cleavage-caspase-3 (1:500; Cell Signaling), Aurora A (1:1000; Cell Signaling), NOXA (1:1000; Millipore), Mcl-1 (1:1000; Cell Signaling), Bcl-2 (1:1000; Cell Signaling), Bcl-xL (1:1000; Cell Signaling), CycB1 (1:1000; Cell Signaling), p-Histone 3 (1:500; Cell Signaling) and β-actin (1:5000; Sigma).

ATPlite assay

Cells were transfected with indicated plasmids or siRNA and seeded into 96-well in triplicate; or cells were seeded into 96-well plates in triplicate and then treated with indicated compounds for indicated time. Cells finally were collected at indicated time for the ATPlite assay (Perkin-Elmer), according to the manufacturer's instructions.

Annexin V-FITC apoptosis analysis

An Annexin V assay was performed according to the manufacturer's instructions (FITC Annexin V Apoptosis Detection Kit I, BD Pharmingen). Briefly, approximately 5×10^5/mL cells in 6-well plates were treated with various concentrations of the indicated compounds. The cells were harvested and used for Annexin V-FITC/PI staining. The percentage of apoptotic cells was determined using FACS flow cytometer equipped with Cell Quest software (BD Immunocytometry Systems).

Cell cycle analysis

For the induction of cell cycle arrest and apoptosis by ZM, MLN8237, and/or ABT-263, approximately 5×10^5/ mL cells in 6-well plates were treated with various concentrations of compounds for 48 h. Cells were collected and fixed in ice-cold 70% ethanol overnight, labeled with 500 μL propidium iodide (50 μL/ mL; Sigma-Aldrich) for at least 15 min in dark at room temperature (RT), and analyzed directly on a Beckon Dickinson FACScan (Oxford). The Sub G1 peak was utilized as a measure of apoptosis.

DNA fragmentation assay

Cells were seeded into 100-mm dishes at 1×10^6 cells per dish, followed by treated with ZM for 48 h. The cells were then harvested by scraping, pelleted and lysed in 600 μL of lysis buffer (5 mM Tris-HCl, pH 8, 20 mM EDTA and 0.5% Triton X-100). The fragmented DNAs in the supernatant after 14,000 rpm centrifugation were extracted with PCI (Phenol/Chloroform/Isopropanol) (Fisher) and precipitated with ethanol, followed by electrophoresis in a 1.8% agarose gel.

siRNA, and transfection

The siRNAs sequence targeting CycG1 is 5'-TGGCCTCAGAATGACTGCAAGACTA-3' [23] and sequence targeting NOXA is 5'-GGTGCACGTTTCATCAATTTG-3'. The sequence for the scrambled control siRNA is 5'-AUUGUAUGCGAUCGCAGACUU-3' [24]. Transfection of siRNAs was carried out using Lipofectamine 2000 (Invitrogen).

Patients and Immunohistochemical (IHC) staining

The human TNBC tissue microarrays were described previously in our study [25]. IHC staining of human lung cancer TMAs was performed as described previously [26]. For the assessment of CycG1, the staining intensity was scored as follows: negative (score 0), bordering (score 1), weak (score 2), moderate (score 3), and strong (score 4); staining extent was graded into five parts according to the percentage of elevated staining cells in the field: negative (score 0), 0-25% (score 1), 26-50% (score 2), 51-75% (score 3) and 76-100% (score 4). Then expression of CycG1 was evaluated by combined assessing of staining intensity and extent. IHC staining was assessed and scored by two independent pathologists (Xu J and Zhang WF), who were blinded to the clinicopathological data.

Selection of a cutoff score for CycG1 expression

The ROC curve analysis was subjected to the selection of CycG1 cutoff score for overall survival (OS) and progression-free survival (PFS) as described previously [26]. Briefly, the sensitivity and specificity for the outcome being studied at each score of the three proteins were plotted to generate ROC curves. The

score localized closest to the point at both maximum sensitivity and specificity (0.0, 1.0) on the curve, was selected as the cutoff score leading to the greatest number of tumors which were classified as having or not having the outcome. To facilitate ROC curve analysis, the patient outcome features were dichotomized by survival [death vs. other outcome (censored, alive, or death from other causes)].

Cloning of HA-CycG1 and –Mcl-1 constructs

To clone wild-type CycG1, the human cDNA was PCR-amplified using the primers 5'-GCG GCC GCA TGA TAG AGG TAC TGA CAA CAA CTG-3' and 5'-CTC GAG TTA AGG GAC CAT TTC AGG AAT TGT TGG-3', and then cloned into pcDNA-HA_3 using Not1 and Xho1 sites. The primers for cloning wild-type Mcl-1 are 5'-GAA TTC ATG TTT GGC CTC AAA AGA AAC GCGG-3' and 5'-AAG CTT CTA TCT TAT TAG ATA TGC CAA ACC AGCTC-3' and then cloned into pcDNA3-HA_3 using EcoR1 and HidIII sites.

Statistical analysis

Statistical analysis was performed using SPSS version 20.0 (SPSS Inc.). Student's t-test was used to make a statistical comparison between groups. The level of significance was set at $P < 0.05$. Both Calcusyn software (Biosoft, Ferguson, MO, USA) [27, 28] and Jin's formula [29] were used to evaluate the synergistic effects of drug combinations. Jin's formula is given as: $Q = Ea+b/(Ea + Eb – Ea \times Eb)$, where Ea+b represents the cell proliferation inhibition rate of the combined drugs, while Ea and Eb represent the rates for each drug respectively. A value of Q = 0.85-1.15 indicates a simple additive effect, while Q > 1.15 indicates synergism. Combination index (CI) plots were generated using CalcuSyn software. A value of CI < 1 indicates synergism.

Results

Aurora kinase inhibitor ZM447439 induces apoptosis-resistant polyploidy in CycG1-amplified breast cancer cells

CycG1 is overexpressed in breast cancer cells [11], and overexpression of CycG1 promotes cell survival after paclitaxel exposure by inducing mitotic slippage first and then polyploidy in multiple cancer cells [21], indicating that CycG1 is a potential oncogenic target. Recently, we found that Aurora kinase inhibitor ZM induced mitotic slippage and resistant polyploidy in acute myeloid leukemia cells [30]. We further found that pan-Aurora kinase (-A and -B) inhibitor ZM [31], but not Aurora A inhibitor MLN8237 [32, 33], induced polyploidy in breast cancer (for all online suppl. material, see www.karger.com/doi/10.1159/000480322, Fig. S1A). Herein, we try to identify the crosstalk between CycG1 and ZM-induced polyploidy in breast cancer.

We firstly detected the endogenous expression of CycG1 in multiple breast cancer cells, and found that CycG1 was highly expressed in ZR-75-1 (Luminal), MDA-MB-468 (TNBC), and MDA-MB-231 (TNBC), whereas lowly expressed in SKBR3 (Luminal), MCF7 (Luminal), and MDA-MB-361 (Luminal) breast cancer cells (Fig. 1A), indicating that CycG1 is mainly elevated in TNBC cells, which is one of the most aggressive types in breast cancer [25, 34]. All the six cell lines were then treated with ZM for 48 h, and detected by ATPlite assay. ZM showed significant cell growth inhibition in MDA-MB-361 (IC50 = 0.3464 μM), MCF7 (IC50 = 0.7815 μM) and SKRB3 (IC50 = 0.9899 μM) cell lines, whereas less inhibition in ZR-75-1 (IC50 = 7.742 μM), MDA-MB-231 (IC50 = 14.31 μM), and MDA-MB-468 (IC50 = 3.246 μM) cell lines (Fig. 1B). We then chose MDA-MB-231, MCF7, ZR-75-1 and MDA-MB-361 cell lines for next experiments. We firstly determined the cell cycle distribution upon ZM treatment in the four cell lines. We found that ZM treatment induced apoptosis in MCF7 (Sub G1: 8.57% at 5 μM; 18.27% at 10 μM) and MDA-MB-361 (Sub G1: 7.35% at 5 μM; 10.14% at 10 μM) cell lines (Fig. 1C & D), which show low CycG1 expression, whereas induced polyploidy with few apoptosis in MDA-MB-231 (4N 6.98%+8N 0% at 0 μM; 4N 58.26%+8N 14% at 5 μM; 4N 65.04%+8N 21.59% at 10 μM) and ZR-75-1 (4N 30.76% +8N 0% at 0 μM; 4N 60.23% +8N 14.05% at 5 μM; 4N 64.81%+8N 21.33% at 10 μM) cell lines (Fig. 1C & D), which show high CycG1 expression.

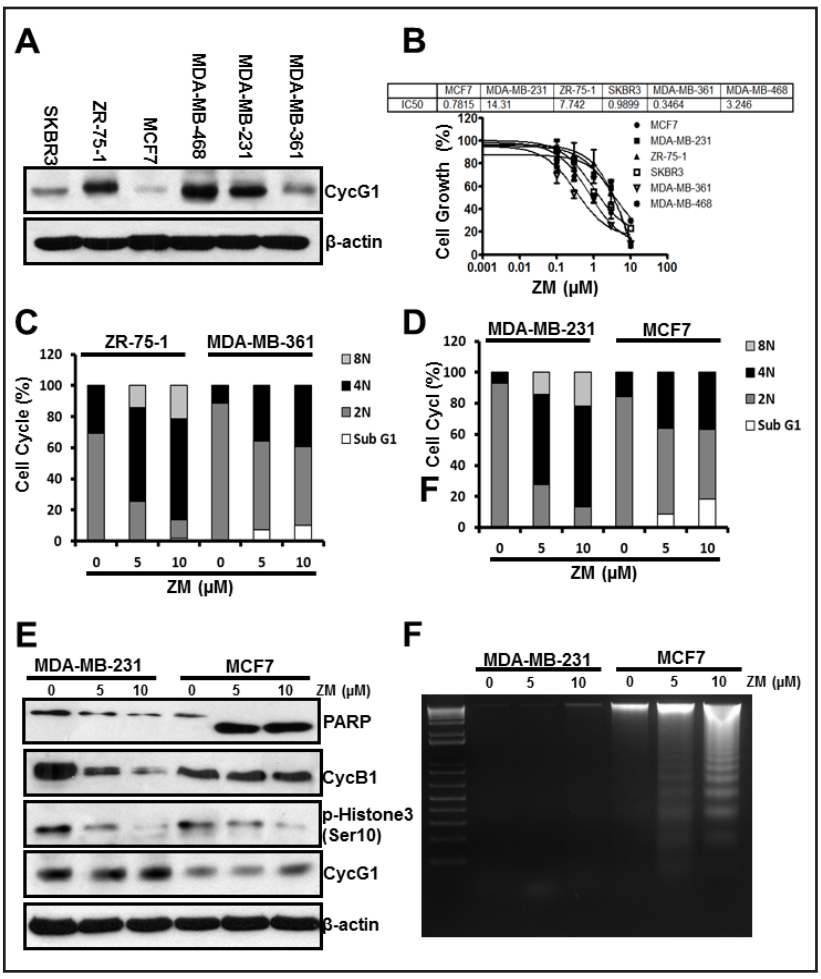

Fig. 1. Aurora kinase inhibitor ZM447439 induces resistant polyploidy in CycG1-amplified breast cancer cells. (A) CycG1 expression in multiple breast cancer cell lines. Breast cancer cells were collected for IB by using the indicated antibodies. (B) Cell growth inhibition of ZM in multiple breast cancer cell lines. Cells (5000 cells/well) were treated with DMSO or different doses of ZM for 48 h. ATPlite assay was performed to detect the cell viability as described in "Material and Methods". (C&D) Cell cycle distribution upon ZM treatment in breast cancer cells. ZR-75-1 and MDA-MB-361 (C) or MDA-MB-231 and MCF7 (D)were treated with DMSO or different doses of ZM for 48 h. Cells were then collected for propidium iodide staining and flow cytometry. Percentages of the cell population of Sub G1, 2N, 4N, 8N, were shown. (E&F) ZM treatment inhibits apoptosis in MDA-MB-231 but induces apoptosis in MCF cells. Cells were treated with DMSO or different doses of ZM for 48 h, followed by IB (E) and DNA fragmentation (F).

To further demonstrate the mechanism by which ZM induces polyploidy in CycG1-amplified breast cancer cells, we detected CycB1, a key mitotic progression marker, and the apoptotic protein PARP upon ZM treatment in breast cancer cells. We found that ZM treatment failed to induce an increase of cleveage PARP and resulted in a dose-dependent degradation of CycB1 in CycG1-amplifed MDA-MB-231 and ZR-75-1 cell lines, whereas triggered significant increase of cleveage PARP in CycG1-low-expressed MCF7 and MDA-MB-361 cells (Fig. 1E, and see supplementary material, S1B). However, ZM treatment did not show any effects on CycG1 expression in the four cell lines, but really caused a decrease of phosphorylation of histone H3 at Ser10 (Fig. 1E, and see supplementary material, S1B), which is phosphorylated by Aurora kinase *in vivo* [31, 35], accordingly indicating an inhibition of Aurora kinase by ZM. DNA fragmentation assay further demonstrated that ZM treatment selectively triggered apoptosis in MCF7 and MDA-MB-361 cells (Fig 1F, and see supplementary material, S1C). Above data indicate that ZM induces mitotic slippage (degradation of CycB1) and apoptosis-resistant polyploidy in CycG1-amplified breast cancer cells.

CycG1 overexpression promotes but siRNA silencing inhibits ZM-induced polyploidy cells

To further confirm that CycG1 is a crucial factor to enhance ZM-induced resistant polyploidy cells, we firstly transfected HA-CycG1 into CycG1-low-expressed MCF7 and MDA-MB-361 cells and found that exogenously expressed CycG1 promoted cell proliferation

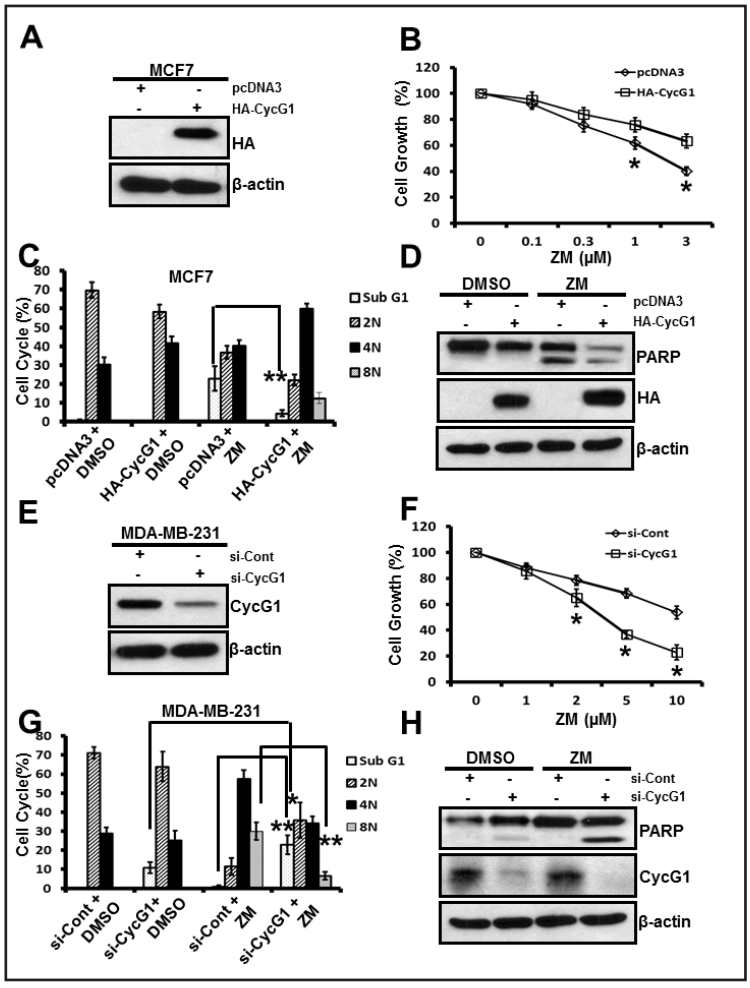

Fig. 2. CycG1 overexpression promotes and RNAi silencing suppresses polyploidy upon ZM treatment. (A&B) Overexpression of CycG1 promotes cell proliferation in MCF7 cells. MCF7 cells were transfected with pcDNA3 or HA-CycG1, followed by IB and ATPlite assay. (C&D) Overexpression of CycG1 suppresses apoptosis and enhances ZM-induced polyploidy cells upon ZM treatment. MCF7 cells were transfected with pcDNA3 or HA-CycG1 and then treated with DMSO or ZM for 24 h, followed by propidium iodide staining and flow cytometry (C), as well as IB (D). Shown are mean ± SD; **, P < 0.01. (E&F) CycG1 RNAi silencing suppresses cell growth in MDA-MB-231 cells. MDA-MB-231 cells were transfected with si-Cont or si-CycG1, followed by IB and ATPlite assay. (G&H) CycG1 silencing triggers apoptosis and blocks ZM-induced polyploidy cells. MDA-MB-231 cells were transfected with si-Cont or si-CycG1 and then treated with DMSO or ZM for 24 h, followed by propidium iodide staining and flow cytometry (G), as well as IB (H). Shown are mean ± SD; *P < 0.05; **, P < 0.01.

in both cell lines (Fig. 2A-B, and see supplementary material, S2A-B). While ZM induced apoptosis in MCF7 and MDA-MB-361 cells, overexpression of CycG1 did not only block the apoptosis, demonstrated by decrease of Sub G1 (22.91% VS. 4.47% in MCF7, P < 0.01 and 23.9% VS 4.81% in MDA-MB-361, P<0.01; Fig. 2C, and see supplementary material, S2C) and cleavage PARP (Fig. 2D, and see supplementary material, S2D), but also trigger the occurrence of polyploidy (Fig. 2C, and see supplementary material, S2C). We also silenced CycG1 in MDA-MB-231 and ZR-75-1 cells and found that CycG1 deletion significantly suppressed cell proliferation in the two cell lines (Fig. 2E-F, and see supplementary material, S2E-F). Additionally, when ZM treatment caused apoptosis-resistant polyploidy in both of the cell lines, CycG1 silencing could block ZM-induced polyploidy (30% VS. 6.54% in MDA-MB-231, P < 0.01; 25.7% VS. 4.88% in ZR-75-1, P < 0.01) and induce apoptosis (Fig. 2G-H, and see supplementary material, S2G-H). These results convincingly show that CycG1 amplification contributes to the resistant polyploidy upon ZM treatment in breast cancer cells.

Bcl-xL inhibition elicits synergistic cytotoxicity in combination with ZM

Previous [36] and our recent study [30] reported that ABT-263, a small-molecule BH3 mimetic that inhibits Bcl-xL, Bcl-2, and Bcl-w, blocked Aurora kinase inhibitor-induced polyploidy and resulted in cell apoptotic death. Here, we combined ZM with ABT-263 in CycG1-amplified breast cancer cells and found that combination of two compounds significantly

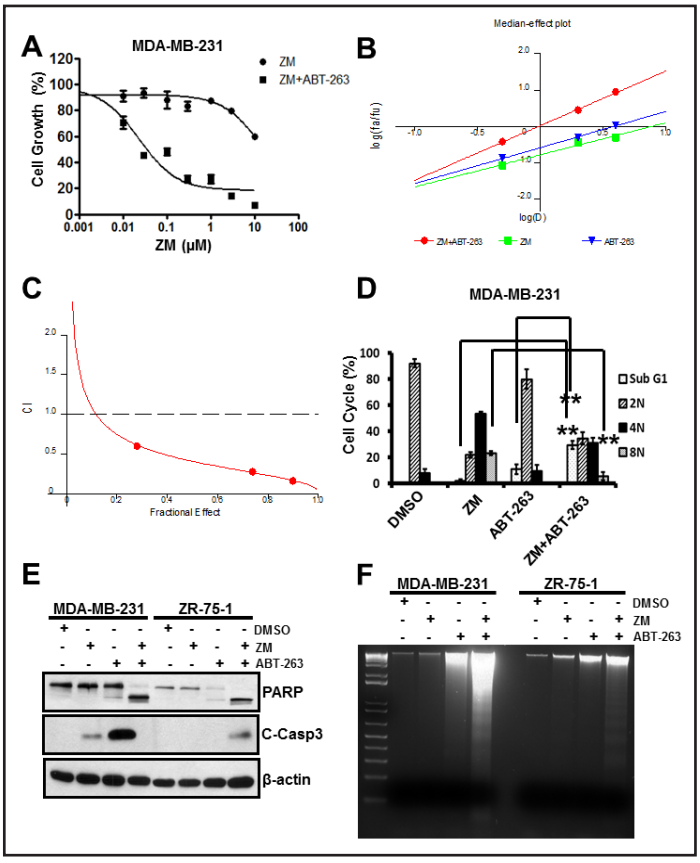

Fig. 3. ZM in combination with ABT-263 elicits synergistic cytotoxicity. (A) MDA-MB-231 Cells (5000 cells/well) were treated with different doses of ZM or combination of different dozes of ZM with ABT-263 (1 μM) for 48 h, followed by ATPlite assay. (B&C) ZM and ABT-263 synergistically inhibit cell proliferation in MDA-MB-231 cells. CI-effect plots and median effect plots were generated using CalcuSyn software. The points a, b, and c represent CI values for the combinations 0.5, 1, and 2 μM ZM with 0.5, 1, and 2 μM ABT-263 in a constant ratio, respectively. (D) ABT-263 blocks ZM-induced polyploidy. MDA-MB-231 cells were incubated with DMSO, ZM (5 μM), and/or ABT-263 (1 μM) for 48 h; cells were then collected, fixed with ice-cold 70% ethanol overnight, and collected for propidium iodide staining and flow cytometry. Shown are mean ± SD, **P < 0.01. (E&F) ABT-263 triggers apoptosis in ZM-induced polyploidy cells. MDA-MB-231 and ZR-75-1 cells were treated with DMSO, ZM (5 μM), and/or ABT-263 (1 μM) for 48 h; cells were then harvested for IB with indicated antibodies (E) or for DNA fragmentation assay (F).

inhibited cell growth compared with ZM single treatment (Fig. 3A, and see supplementary material, S3A). Next, both CalcuSyn software [27, 28] and Jin's formula [29] were used to determine the synergy of the two agents. MDA-MB-231 and ZR-75-1 cells were cultured with combinations of these two drugs at different doses but in a constant ratio (ZM to ABT-263: 0.5 μM to 0.5 μM, 1 μM to 1 μM, and 2 μM to 2 μM, respectively) for 48 h. The combination of 0.5 μM ZM with 0.5 μM ABT-263 in MDA-MB-231 cells inhibited cell proliferation by 28%, compared with mono-therapy of ZM by 8.0% or ABT-263 by 12.0%, indicating synergism (CI = 0.606; Q = 1.47; Fig. 3B & C). Escalating doses, i.e. co-treatment with 1 μM ZM and 1 μM ABT-263 (CI = 0.281; Q = 1.43) or 2 μM ZM and 2 μM ABT-263 (CI = 0.165; Q = 1.2), show synergetic effects in MDA-MB-231 cells (Fig. 3B & C). Combination of ZM and ABT-263 also showed synergistic effects in ZR-75-1 cells (0.5 μM ZM and 0.5 μM ABT-263: CI = 1.140 and Q = 0.97; 1 μM ZM and 1 μM ABT-263: CI = 0.633 and Q = 1.18; 2 μM ZM and 2 μM ABT-263: CI = 0.336 and Q = 1.28) (see supplementary material, Fig. S3B & C).

Cell cycle distribution further showed that ZM mono-therapy induced huge polyploidy cells (51.78% 4N and 26.4% 8N) that were blocked significantly in combination with ABT-263 (31.02% 4N and 5.24% 8N; P < 0.01) and addition of ABT-263 triggered rapid apoptosis in polyploidy cells as seen by an increase in Sub G1 from 1.83% (ZM alone) to 29.34% (combination of ZM and ABT-263; P<0.01) (Fig. 3D). Combination of ABT-263 with ZM also blocked polyploidy cells and induced apoptosis in ZR-75-1 cells (see supplementary material, Fig. S3D), although the effect was lower than that in MDA-MB-231 cells. Furthermore, combination ZM with ABT-263 induced significant increase of the pro-apoptotic cleavage PAPR and Caspase 3 (C-Casp3) (Fig. 3E), as well as significant apoptotic cell death in a DNA fragmentation assay (Fig. 3F). These data demonstrate that ZM induces polyploidy cells, which can be blocked by ABT-263, in CycG1-amplified breast cancer cells.

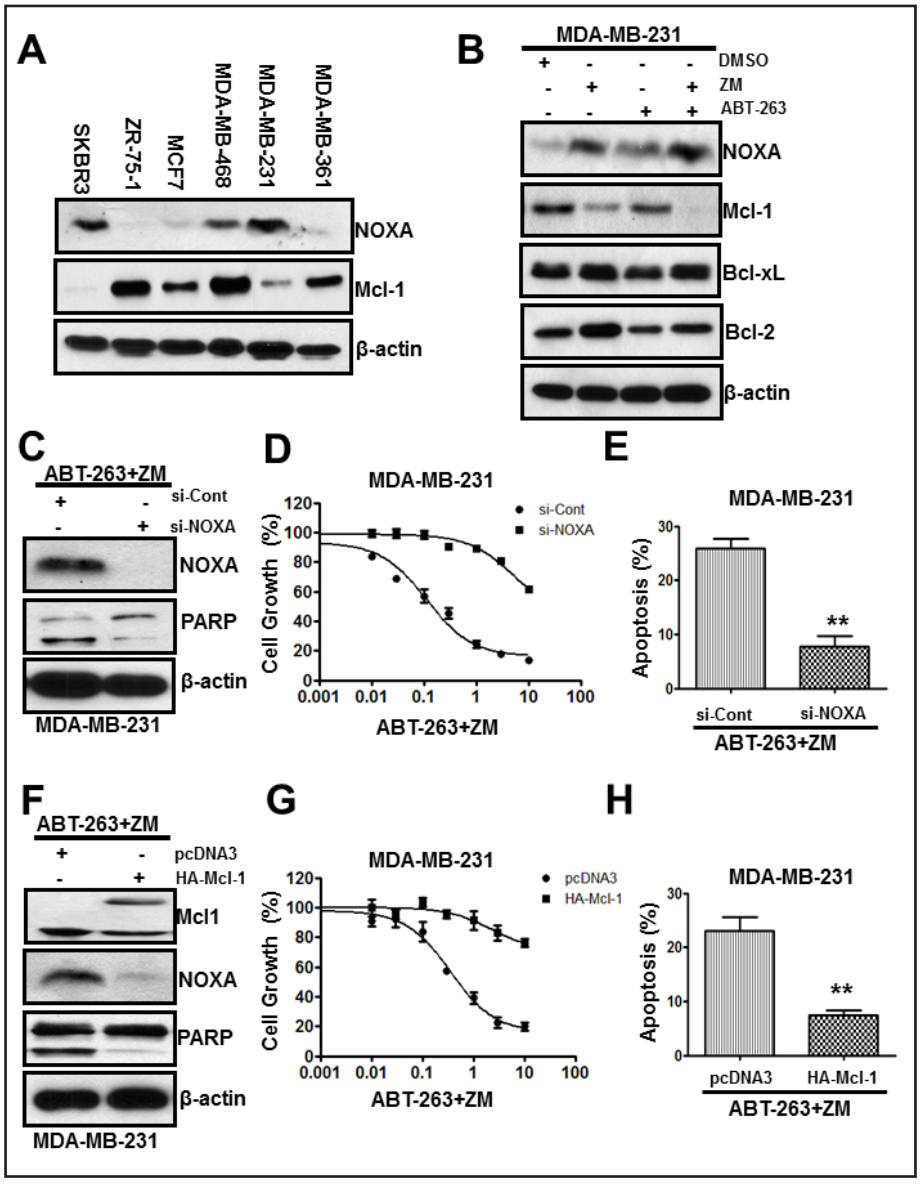

Fig. 4. CycG1-amplified breast cancer cells are sensitive to ABT-263 due to NOXA expression. (A) Co-expression of NOXA and Mcl-1 in multiple breast cancer cell lines. Multiple breast cancer cells were collected for IB assay with indicated antibodies. (B) ZM treatment decreases Mcl-1 and increases NOXA in CycG1-amplyfied breast cancer cells. MDA-MB-231 cells were treated with DMSO, ZM (5 μM), and/or ABT-263 (1 μM) for 48 h, followed by IB with indicated antibodies. (C-E) Apoptosis caused by combination of ABT-263 and ZM in CycG1-amplyfied cells is blocked by NOXA deletion. MDA-MB-231 cells were treated with ABT-263 and ZM and then transfected with si-Cont or si-NOXA, followed by IB (C), ATPlite assay (D), and Annexin V-FITC apoptosis assay (E). (F-H) Apoptosis caused by combination of ABT-263 and ZM in CycG1-amplyfied cells is blocked by overexpression of Mcl-1. MDA-MB-231 cells were treated with ABT-263 and ZM and then transfected with pcDNA3 vector or HA-Mcl-1, followed by IB (F), ATPlite assay (G), and Annexin V-FITC apoptosis assay (H).

Synergistic effects caused by ZM and ABT-263 combination are due to high NOXA expression

We next determine why ZM and ABT-263 combination shows synergy in CycG1-amplified breast cancer cells, especially in MDA-MB-231 cells. Previous studies reported that high levels of NOXA confers sensitivity to Bcl-2/Bcl-xL inhibitors [37-39], and exogenous expression of NOXA sensitized cancer cells to Bcl-2/Bcl-xL inhibitors [38]. We accordingly suggest that increased NOXA expression may contribute to ABT-263 sensitivity observed in CycG1-amplified breast cancer cells. We firstly detected the expression of NOXA and its inhibitor Mcl-1 in breast cancer cell lines, and observed a negative relationship between NOXA and Mcl-1 (Fig. 4A). Intriguingly, NOXA shows higher expression in MDA-MB-231 cells

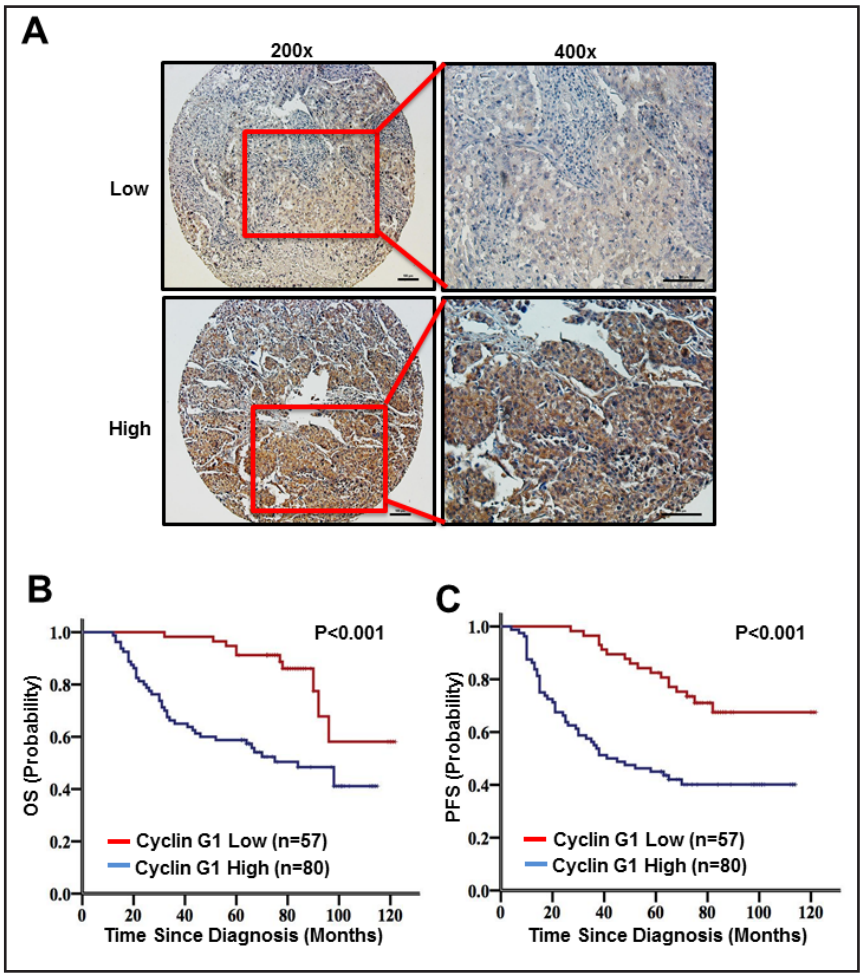

Fig. 5. CycG1 overexpression in TNBC patients predicts an inferior prognosis. (A) CycG1 staining in TNBC tissues: TNBC tissue microarrays were stained by using Abs against CycG1 (Santa Cruz). (B&C) Kaplan–Meier curves to show the association between the levels of CycG1 expression and overall survival (B), as well as progression-free survival (C) of patients with TNBC.

than that in ZR-75-1 cells, explaining why ABT-263 shows significant growth inhibition and apoptosis in MDA-MB-231.

Previous study reported that Mcl-1 was decreased but NOXA was increased during the polyploidization process induced by Aurora kinase inhibitor [36]. We further demonstrated that ZM treatment increased NOXA but decreased Mcl-1 in both of MDA-MB-231 and ZR-75-1 cell lines, with mild increase of the other two Bcl-2 family proteins Bcl-2 and Bcl-xL (Fig. 4B, and see supplementary material, S4A). We then try to demonstrate the above findings by using two rescue experiments. MDA-MB-231 and ZR-75-1 cells were firstly treated by combination of ZM and ABT-263, which causes accumulation of NOXA, followed by silencing of NOXA. We found that ABT-263 and ZM combination inhibited cell proliferation and induced apoptosis significantly, which could be blocked by NOXA siRNA silencing as demonstrated by the increase of cell growth, and decrease of cleavage PARP and cell apoptosis (25.9% VS. 7.8% in MDA-MB-231; 21.9% VS. 7.4% in ZR-75-1; $P < 0.01$) (Fig. 4C-E, and see supplementary material, S4B-D). Consistently, ectopic expression of Mcl-1 leads to decrease of NOXA and then also inhibits cell growth and apoptosis caused by ZM and ABT-263 combination (Fig. 4F-H, and see supplementary material, SE-G). Collectively, ZM-triggered polyploidization induces apoptosis effectors while compromising Mcl-1 function, may directly via down-regulation of Mcl-1 and/or indirectly by up-regulation of NOXA.

CycG1 is an inferior prognostic factor for paclitaxel-treated TNBC patients

In Fig. 1A, we found that CycG1 was mainly elevated in TNBC cells, which is one of the most aggressive types in breast cancer. Furthermore, CycG1 overexpression induces polyploidy and promotes cell survival after paclitaxel exposure, as well as predicts significantly shorter

post-surgical survival in patients with ovarian cancer who have received adjuvant chemotherapy with taxanes [21]. Here, we enrolled 137 TNBC patients [26] , which were treated with adjuvant chemotherapy with paclitaxel, and determined the prognostic role of CycG1 in these patients. We performed immunohistochemistry (IHC) staining to measure the CycG1 level in a TNBC tissue microarray, and scored results using receiver operating characteristic (ROC) curve analysis [26]. As shown in (see supplementary material) Suppl. Fig. S5A and B, the CycG1 cutoff score was 4.8 ($P < 0.001$) for OS and 4.6 ($P < 0.001$) for PFS. We therefore divided the cohort into high (score ≥ 4) and low (score < 4) expression based on the cutoff points.

Table 1. Characteristics of 137 TNBC patients

Variable	All cases	CyclinG1		
		High expression	Low expression	*P*
Age (Years)				
≥48.00	54	32	22	1.000
<48.00	83	48	35	
Family history				
Yes	18	6	12	0.038
No	119	74	45	
Pathologic characteristics				
Invasive ductal carcinoma	131	76	55	1.000
Others	6	4	2	
Lymph node status				
Negative	64	31	33	0.037
Positive	73	49	24	
Initial clinical stage				
I	13	3	10	0.001
II	59	27	32	
III	65	50	15	
Tumor stage				
T1+T2	81	35	46	0.001
T3+T4	56	45	11	
Adjuvant radiotherapy				
Yes	34	22	12	0.428
No	103	58	45	
Adjuvant chemotherapy				
Yes	121	70	51	0.793
No	16	10	6	
Recurrence				
Local	37	25	12	0.001
Distant	47	39	8	
No	53	16	37	

Clinical features of the 137 TNBC patients, including age, family history, pathological characteristics, lymph node status, initial clinical stage, tumor stage, adjuvant radiotherapy, adjuvant chemotherapy, and recurrence, were summarized in Table 1. Immunoreactivity of CycG1 was observed primarily in the cytoplasm, with occasionally yellowish brown granules seen in the nuclei (Fig. 5A). In the cohort of 137 TNBC patients, high expression of CycG1 was examined in 80 of 137 (58.4%) patients and low expression of CycG1 was examined in 57 of 137 (41.6%) patients. CycG1 high expression was positively correlated with family history ($P = 0.038$, Table 1), lymph node status ($P = 0.037$, Table 1), initial clinical state ($P = 0.001$, Table 1), tumor stage ($P = 0.001$, Table 1), and the recurrence rate ($P = 0.001$, Table 1) in TNBC patients. Furthermore, our results showed that patients with CycG1 high expression had a significantly inferior OS (median survival time: 84 months VS. 122 months, $P < 0.001$, Fig. 5B) and PFS (median survival time: 42 months VS. 122 months, $P < 0.001$, Fig. 5C) than those with CycG1 low expression, indicating that CycG1 is a poor prognostic biomarker in TNBC patients treated with paclitaxel.

Discussion

Polyploidy, a state in which cells possess more than two complete sets of homologous chromosomes, commonly originates from cell fusion or cytokinesis [18], as well as occurs from mitotic slippage induced by SAC-dissatisfaction [40, 41]. Slippage occurs if CycB1 levels fall below the mitotic exit threshold before the generation of sufficient death signals, whereas cell death occurs if sufficient death signals accumulate before CycB1 is adequately degraded [41]. Thus, mitotic slippage and apoptosis can be viewed as two competing pathways. Previous studies report that CycG1, an atypical one of the cyclin family, is highly expressed in cancer cells and induces mitotic arrest firstly, but eventually undergo slippage to exit mitosis, promoting cell survival after paclitaxel exposure [21]. Here, we also found that Aurora kinase inhibitor ZM induced polyploidy cells via mitotic slippage and inhibited

apoptosis in CycG1-amplified breast cancer cells, whereas triggered apoptosis in CycG1-low-expressed cells (Fig. 1, see supplementary material, S1). Furthermore, ectopic expression of CycG1 promoted ZM-induced polyploidy cells and inhibited apoptosis, but deletion of CycG1 showed the opposite effects (Fig. 2). Consistent with the previous findings, CycG1 tends to be an oncogenic target and associates with the resistance of targeted inhibitor treatment.

Amplification of CycG1 is the driving oncogenic event in a subset of cancer types [11-14]; exposure to CycG1 antisense oligonucleotides results in tumor growth inhibition [8-10], further validating CycG1 as an important target. As a non-kinase, however, drugging CycG1 with small molecule inhibitors has proven challenging. Recently, MicroRNAs (miRNAs) has been reported to negatively regulate CycG1 expression and suppresses tumorigenesis and tumor growth. MiR-23b, binding with the 3′ untranslated region of CycG1, down-regulated CycG1 mRNA and protein expression, inhibiting ovarian cancer tumorigenesis and progression [23]. CycG1 was also found to be a target of miR-122 [42], which, via down-regulation of CycG1, can trigger apoptosis and increase sensitivity of HCC-derived cells to doxorubicin [23], hence providing the biological basis toward the development of combined chemo- and CycG1-targeted therapy.

Accumulated evidences show that drug resistance could be reversed by single compound or combination of compounds targeting different pathways. β-Elemene reversed chemoresistance by reducing resistance transmission via exosomes [43], and Cinnamaldehyde Derivative (CB-PIC) sensitized resistant cancer cells to drug-induced apoptosis via inhibition of STAT3 and AKT signaling [44]. Combination of two chemotherapeutics C9 and Dichloroacetate (DCA) showed synergistic effects in breast cancer cells through ROS-JNK-Bcl-2 pathways [45]. Recently, ABT-263, a BH3 mimetic, has been demonstrated to inhibit Aurora kinase inhibitor-induced polyploidy and produces a synergistic loss of viability in a range of cancer cell lines when combination with Aurora B inhibitors [30, 36]. In this study, we also identify that ATB-263 triggers apoptosis in ZM-induced polyploidy cells and combination of the two compounds shows significant synergistic effects in CycG1-amplified breast cancer cells. Indeed, neutralization of Bcl-xL/Bcl-2 is not normally sufficient to trigger apoptosis in diploid or aneuploidy cells derived from most solid tumors [46]. We then dig out two important findings that can explain the synergistic effects of the two compounds in CycG1-amplified breast cancers. Firstly, MDA-MB-231 shows higher endogenous NOXA expression than ZR-75-1, which is consistent with the previous findings that high NOXA expression confers sensitivity to Bcl-2/Bcl-xL inhibitors [37-39]. Secondly, ZM treatment down-regulated Mcl-1 and enhanced its antagonist NOXA, with subtle increase of Bcl-2 and Bcl-xL in CycG1-amplified breast cells. Down-regulation of Mcl-1 and up-regulation of NOXA are common responses to polyploidization in cancer cell lines [36]. Collectively, ZM-triggered polyploidization induced apoptosis effectors while compromising Mcl-1 function, directly via down-regulation of Mcl-1 and/or indirectly by up-regulating Noxa. However, cell viability is still maintained during this period of ZM-induced polyploidization, we infer that the burden to support viability is shifted from Mcl-1 to Bcl-2/-xL. Thus, ABT-263 and ZM combination hold therapeutic utility in CycG1-amplified-induced polyploidy cells.

Breast cancer is one of the leading causes of cancer-related death among adult females in the world. The management and prognosis of breast cancer are largely determined by the expression status of estrogen receptor (ER), progesterone receptor (PR), and human epidermal growth factor receptor 2 (HER2) of the tumor [47-49]. TNBC, defined as a tumor subtype that lack of ER, PR and HER2 expression, shows a poor prognosis due to its aggressive tumor biology and resistance to most available endocrine and molecularly targeted treatments [50-52]. Thus, TNBC presents as a major challenge for the development of effective therapeutic strategies of breast cancer [34]. In the present study, we found that CycG1 is highly expressed in TNBC cell lines, including MDA-MB-231 and MDA-MB-468 cell lines (Fig. 1A), and associated with ZM-induced resistant polyploidy. Furthermore, high expression of CycG1 enhances paclitaxel-induced polyploidy and resistance, and predicts poor post-surgical survival in patients with ovarian cancer treated with taxanes [21]. Here, we demonstrated that CycG1 is overexpressed in TNBC patients who have received adjuvant

chemotherapy with paclitaxel and predicts short OS and PFS, indicating that CycG1 is an inferior prognostic biomarker of TNBC patients receiving adjuvant paclitaxel chemotherapy probably through induction of polyploidy.

In summary, we demonstrate the pro-survival function of CycG1 in cancer polyploidy cells induced by Aurora kinase inhibitor ZM. Combination of Bcl-xL/Bcl-2 inhibitor ABT-263 and ZM produces synergistic anti-proliferative activity *in vitro*. Moreover, CycG1 serves as a poor prognostic biomarker for TNBC patients receiving paclitaxel-based adjuvant chemotherapy and thus, ABT-263/ZM combination hold therapeutic utility in the CycG1-amplified subset of breast cancer and CycG1 is a novel anti-cancer target in breast cancer.

Acknowledgements

This work was financially supported by the National Natural Science Foundation of China (Grant No. 81402495 to WH. Zhou; Grant No. 81402194 to J. Xu).

Disclosure Statement

The authors declare that they have no competing interests.

References

1 Tamura K, Kanaoka Y, Jinno S, Nagata A, Ogiso Y, Shimizu K, Hayakawa T, Nojima H, Okayama H: Cyclin G: a new mammalian cyclin with homology to fission yeast Cig1. Oncogene 1993;8:2113-2118.
2 Okamoto K, Beach D: Cyclin G is a transcriptional target of the p53 tumor suppressor protein. EMBO J 1994;13:4816-4822.
3 Ohtsuka T, Ryu H, Minamishima YA, Ryo A, Lee SW: Modulation of p53 and p73 levels by cyclin G: implication of a negative feedback regulation. Oncogene 2003;22:1678-1687.
4 Okamoto K, Li H, Jensen MR, Zhang T, Taya Y, Thorgeirsson SS, Prives C: Cyclin G recruits PP2A to dephosphorylate Mdm2. Mol Cell 2002;9:761-771.
5 Kimura SH, Ikawa M, Ito A, Okabe M, Nojima H: Cyclin G1 is involved in G2/M arrest in response to DNA damage and in growth control after damage recovery. Oncogene 2001;20:3290-3300.
6 Jensen MR, Factor VM, Fantozzi A, Helin K, Huh CG, Thorgeirsson SS: Reduced hepatic tumor incidence in cyclin G1-deficient mice. Hepatology 2003;37:862-870.
7 Baek WK, Kim D, Jung N, Yi YW, Kim JM, Cha SD, Bae I, Cho CH: Increased expression of cyclin G1 in leiomyoma compared with normal myometrium. Am J Obstet Gynecol 2003;188:634-639.
8 Skotzko M, Wu L, Anderson WF, Gordon EM, Hall FL: Retroviral vector-mediated gene transfer of antisense cyclin G1 (CYCG1) inhibits proliferation of human osteogenic sarcoma cells. Cancer Res 1995;55:5493-5498.
9 Gordon EM, Liu PX, Chen ZH, Liu L, Whitley MD, Gee C, Groshen S, Hinton DR, Beart RW, Hall FL: Inhibition of metastatic tumor growth in nude mice by portal vein infusions of matrix-targeted retroviral vectors bearing a cytocidal cyclin G1 construct. Cancer Res 2000;60:3343-3347.
10 Kampmeier J, Behrens A, Wang Y, Yee A, Anderson WF, Hall FL, Gordon EM, McDonnell PJ: Inhibition of rabbit keratocyte and human fetal lens epithelial cell proliferation by retrovirus-mediated transfer of antisense cyclin G1 and antisense MAT1 constructs. Hum Gene Ther 2000;11:1-8.
11 Reimer CL, Borras AM, Kurdistani SK, Garreau JR, Chung M, Aaronson SA, Lee SW: Altered regulation of cyclin G in human breast cancer and its specific localization at replication foci in response to DNA damage in p53+/+ cells. J Biol Chem 1999;274:11022-11029.
12 Chen DS, Zhu NL, Hung G, Skotzko MJ, Hinton DR, Tolo V, Hall FL, Anderson WF, Gordon EM: Retroviral vector-mediated transfer of an antisense cyclin G1 construct inhibits osteosarcoma tumor growth in nude mice. Hum Gene Ther 1997;8:1667-1674.

13 Perez R, Wu N, Klipfel AA, Beart RW, Jr.: A better cell cycle target for gene therapy of colorectal cancer: cyclin G. J Gastrointest Surg 2003;7:884-889.
14 Wen W, Ding J, Sun W, Fu J, Chen Y, Wu K, Ning B, Han T, Huang L, Chen C, Xie D, Li Z, Feng G, Wu M, Xie W, Wang H: Cyclin G1-mediated epithelial-mesenchymal transition via phosphoinositide 3-kinase/Akt signaling facilitates liver cancer progression. Hepatology 2012;55:1787-1798.
15 Jensen MR, Factor VM, Thorgeirsson SS: Regulation of cyclin G1 during murine hepatic regeneration following Dipin-induced DNA damage. Hepatology 1998;28:537-546.
16 Zhao L, Samuels T, Winckler S, Korgaonkar C, Tompkins V, Horne MC, Quelle DE: Cyclin G1 has growth inhibitory activity linked to the ARF-Mdm2-p53 and pRb tumor suppressor pathways. Mol Cancer Res 2003;1:195-206.
17 Brito DA, Rieder CL: Mitotic checkpoint slippage in humans occurs via cyclin B destruction in the presence of an active checkpoint. Curr Biol 2006;16:1194-200.
18 Ganem NJ, Storchova Z, Pellman D: Tetraploidy, aneuploidy and cancer. Curr Opin Genet Dev 2007;17:157-62.
19 Weaver BA, Cleveland DW: Decoding the links between mitosis, cancer, and chemotherapy: The mitotic checkpoint, adaptation, and cell death. Cancer cell 2005;8:7-12.
20 Rieder CL, Maiato H: Stuck in division or passing through: what happens when cells cannot satisfy the spindle assembly checkpoint. Dev Cell 2004;7:637-651.
21 Russell P, Hennessy BT, Li J, Carey MS, Bast RC, Freeman T, Venkitaraman AR: Cyclin G1 regulates the outcome of taxane-induced mitotic checkpoint arrest. Oncogene 2012;31:2450-2460.
22 Liu Z, Yue S, Chen X, Kubin T, Braun T: Regulation of cardiomyocyte polyploidy and multinucleation by CyclinG1. Circ Res 2010;106:1498-1506.
23 Fornari F, Gramantieri L, Giovannini C, Veronese A, Ferracin M, Sabbioni S, Calin GA, Grazi GL, Croce CM, Tavolari S, Chieco P, Negrini M, Bolondi L: MiR-122/cyclin G1 interaction modulates p53 activity and affects doxorubicin sensitivity of human hepatocarcinoma cells. Cancer Res 2009;69:5761-5767.
24 Zhou W, Xu J, Zhao Y, Sun Y: SAG/RBX2 is a novel substrate of NEDD4-1 E3 ubiquitin ligase and mediates NEDD4-1 induced chemosensitization. Oncotarget 2014;5:6746-6755.
25 Xu J, Wu X, Zhou WH, Liu AW, Wu JB, Deng JY, Yue CF, Yang SB, Wang J, Yuan ZY, Liu Q: Aurora-A identifies early recurrence and poor prognosis and promises a potential therapeutic target in triple negative breast cancer. PloS one 2013;8:e56919.
26 Zhou WH, Tang F, Xu J, Wu X, Yang SB, Feng ZY, Ding YG, Wan XB, Guan Z, Li HG, Lin DJ, Shao CK, Liu Q: Low expression of Beclin 1, associated with high Bcl-xL, predicts a malignant phenotype and poor prognosis of gastric cancer. Autophagy 2012;8:389-400.
27 Chou TC: Theoretical basis, experimental design, and computerized simulation of synergism and antagonism in drug combination studies. Pharmacol Rev 2006;58:621-681.
28 Cai JJ, Qi ZX, Chen LC, Yao Y, Gong Y, Mao Y: miR-124 suppresses the migration and invasion of glioma cells *in vitro* via Capn4. Oncol Rep 2016;35:284-290.
29 Jin ZJ: [Addition in drug combination (author's transl)]. Zhongguo yao li xue bao 1980;1:70-76.
30 Zhou W, Xu J, Gelston E, Wu X, Zou Z, Wang B, Zeng Y, Wang H, Liu A, Xu L, Liu Q: Inhibition of Bcl-xL overcomes polyploidy resistance and leads to apoptotic cell death in acute myeloid leukemia cells. Oncotarget 2015;6:21557-21571.
31 Ditchfield C, Johnson VL, Tighe A, Ellston R, Haworth C, Johnson T, Mortlock A, Keen N, Taylor SS: Aurora B couples chromosome alignment with anaphase by targeting BubR1, Mad2, and Cenp-E to kinetochores. J Cell Biol 2003;161:267-280.
32 Gorgun G, Calabrese E, Hideshima T, Ecsedy J, Perrone G, Mani M, Ikeda H, Bianchi G, Hu Y, Cirstea D, Santo L, Tai YT, Nahar S, Zheng M, Bandi M, Carrasco RD, Raje N, Munshi N, Richardson P, Anderson KC: A novel Aurora-A kinase inhibitor MLN8237 induces cytotoxicity and cell-cycle arrest in multiple myeloma. Blood 2010;115:5202-5213.
33 Xu J, Yue CF, Zhou WH, Qian YM, Zhang Y, Wang SW, Liu AW, Liu Q: Aurora-A contributes to cisplatin resistance and lymphatic metastasis in non-small cell lung cancer and predicts poor prognosis. J Transl Med 2014;12:200.
34 Schneider BP, Winer EP, Foulkes WD, Garber J, Perou CM, Richardson A, Sledge GW, Carey LA: Triple-negative breast cancer: risk factors to potential targets. Clin Cancer Res 2008;14:8010-8018.

35 Long ZJ, Xu J, Yan M, Zhang JG, Guan Z, Xu DZ, Wang XR, Yao J, Zheng FM, Chu GL, Cao JX, Zeng YX, Liu Q: ZM 447439 inhibition of aurora kinase induces Hep2 cancer cell apoptosis in three-dimensional culture. Cell cycle 2008;7:1473-1479.
36 Shah OJ, Lin X, Li L, Huang X, Li J, Anderson MG, Tang H, Rodriguez LE, Warder SE, McLoughlin S, Chen J, Palma J, Glaser KB, Donawho CK, Fesik SW, Shen Y: Bcl-XL represents a druggable molecular vulnerability during aurora B inhibitor-mediated polyploidization. Proc Natl Acad Sci U S A 2010;107:12634-12639.
37 Lucas KM, Mohana-Kumaran N, Lau D, Zhang XD, Hersey P, Huang DC, Weninger W, Haass NK, Allen JD: Modulation of NOXA and MCL-1 as a strategy for sensitizing melanoma cells to the BH3-mimetic ABT-737. Clin Cancer Res 2012;18:783-795.
38 Nakajima W, Hicks MA, Tanaka N, Krystal GW, Harada H: Noxa determines localization and stability of MCL-1 and consequently ABT-737 sensitivity in small cell lung cancer. Cell Death Dis 2014;5:e1052.
39 Wang X, Gu Z, Li G, Zhang S, Cao Z, Yang Z, Liu G: Norcantharidin enhances ABT-263-mediated anticancer activity in neuroblastoma cells by upregulation of Noxa. Oncol Rep 2014;32:716-722.
40 Gascoigne KE, Taylor SS: Cancer cells display profound intra- and interline variation following prolonged exposure to antimitotic drugs. Cancer Cell 2008;14:111-122.
41 Huang HC, Shi J, Orth JD, Mitchison TJ: Evidence that mitotic exit is a better cancer therapeutic target than spindle assembly. Cancer Cell 2009;16:347-358.
42 Gramantieri L, Ferracin M, Fornari F, Veronese A, Sabbioni S, Liu CG, Calin GA, Giovannini C, Ferrazzi E, Grazi GL, Croce CM, Bolondi L, Negrini M: Cyclin G1 is a target of miR-122a, a microRNA frequently down-regulated in human hepatocellular carcinoma. Cancer Res 2007;67:6092-6099.
43 Zhang J, Zhang HD, Yao YF, Zhong SL, Zhao JH, Tang JH: beta-Elemene Reverses Chemoresistance of Breast Cancer Cells by Reducing Resistance Transmission via Exosomes. Cell Physiol Biochem 2015;36:2274-2286.
44 Yun M, Lee D, Park MN, Kim EO, Sohn EJ, Kwon BM, Kim SH: Cinnamaldehyde derivative (CB-PIC) sensitizes chemo-resistant cancer cells to drug-induced apoptosis via suppression of MDR1 and its upstream STAT3 and AKT signalling. Cell Physiol Biochem 2015;35:1821-1830.
45 Stander XX, Stander BA, Joubert AM: Synergistic anticancer potential of dichloroacetate and estradiol analogue exerting their effect via ROS-JNK-Bcl-2-mediated signalling pathways. Cell Physiol Biochem 2015;35:1499-1526.
46 Lin X, Morgan-Lappe S, Huang X, Li L, Zakula DM, Vernetti LA, Fesik SW, Shen Y: 'Seed' analysis of off-target siRNAs reveals an essential role of Mcl-1 in resistance to the small-molecule Bcl-2/Bcl-XL inhibitor ABT-737. Oncogene 2007;26:3972-3979.
47 Prat A, Baselga J: The role of hormonal therapy in the management of hormonal-receptor-positive breast cancer with co-expression of HER2. Nat Clin Pract Oncol 2008;5:531-542.
48 Brenton JD, Carey LA, Ahmed AA, Caldas C: Molecular classification and molecular forecasting of breast cancer: ready for clinical application? J Clin Oncol 2005;23:7350-7360.
49 Sotiriou C, Neo SY, McShane LM, Korn EL, Long PM, Jazaeri A, Martiat P, Fox SB, Harris AL, Liu ET: Breast cancer classification and prognosis based on gene expression profiles from a population-based study. Proc Natl Acad Sci USA 2003;100:10393-10398.
50 Rakha EA, El-Rehim DA, Paish C, Green AR, Lee AH, Robertson JF, Blamey RW, Macmillan D, Ellis IO: Basal phenotype identifies a poor prognostic subgroup of breast cancer of clinical importance. Eur J Cancer 2006;42:3149-3156.
51 Bauer KR, Brown M, Cress RD, Parise CA, Caggiano V: Descriptive analysis of estrogen receptor (ER)-negative, progesterone receptor (PR)-negative, and HER2-negative invasive breast cancer, the so-called triple-negative phenotype: a population-based study from the California cancer Registry. Cancer 2007;109:1721-1728.
52 Gluz O, Liedtke C, Gottschalk N, Pusztai L, Nitz U, Harbeck N: Triple-negative breast cancer--current status and future directions. Ann Oncol 2009;20:1913-1927.